Acta Crystallographica Section F
Structural Biology and Crystallization Communications
ISSN 1744-3091

Preliminary investigation of the three-dimensional structure of *Salmonella typhimurium* uridine phosphorylase in the crystalline state

Maria V. Dontsova,[a] Azat G. Gabdoulkhakov,[b] Olga K. Molchan,[b] Alexandr A. Lashkov,[b] Maria B. Garber,[a] Alexandr S. Mironov,[c] Nadegda E. Zhukhlistova,[b] Ekaterina Yu. Morgunova,[b] Wolfgang Voelter,[d] Christian Betzel,[e] Yang Zhang,[f] Steven E. Ealick[f]* and Al'bert M. Mikhailov[b]*

[a]Institute of Protein Research, Russian Academy of Sciences, Pushchino, Russia, [b]Institute of Crystallography, Russian Academy of Sciences, Moscow, Russia, [c]State Research Institute of Genetic and Selection of Industrial Microorganisms, Moscow, Russia, [d]Institute of Biochemistry and Molecular Biology, University Hospital, c/o DESY, Hamburg, Germany, [e]Institute of Physiological Chemistry, University of Tuebingen, Tuebingen, Germany, and [f]Cornell University, Ithaca, NY, USA

Correspondence e-mail: see3@cornell.edu, amm@ns.crys.ras.ru

Received 7 February 2005
Accepted 8 March 2005
Online 24 March 2005

PDB Reference: StUPh, 1sj9, r1sj9sf.

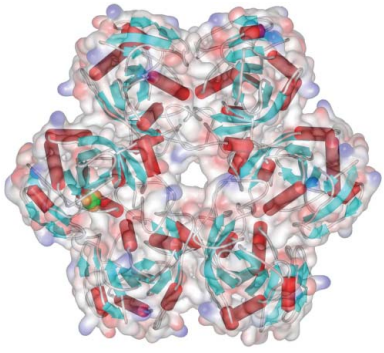

Uridine phosphorylase (UPh) catalyzes the phosphorolytic cleavage of the C—N glycosidic bond of uridine to ribose 1-phosphate and uracil in the pyrimidine-salvage pathway. The crystal structure of the *Salmonella typhimurium* uridine phosphorylase (StUPh) has been determined at 2.5 Å resolution and refined to an R factor of 22.1% and an $R_{\rm free}$ of 27.9%. The hexameric StUPh displays 32 point-group symmetry and utilizes both twofold and threefold non-crystallographic axes. A phosphate is bound at the active site and forms hydrogen bonds to Arg91, Arg30, Thr94 and Gly26 of one monomer and Arg48 of an adjacent monomer. The hexameric StUPh model reveals a close structural relationship to *Escherichia coli* uridine phosphorylase (EcUPh).

1. Introduction

The ability of cells to maintain a constant supply of pyrimidine and purine nucleotides is dependent on both *de novo* synthetic and salvage pathways. The relative importance of either the *de novo* or the salvage pathway in the maintenance of nucleotide pools is variable and dependent on the cell or tissue type. Uridine phosphorylase (UPh; EC 2.4.2.3) is an important enzyme in the pyrimidine-salvage pathway and catalyzes the reversible phosphorolysis of uridine to uracil,

$$\text{uridine} + \text{phosphate} \rightleftharpoons \text{ribose 1-phosphate}.$$

This enzyme is found in most organisms, including human cells. Its level is frequently elevated in tumors. The amino-acid sequence of UPh is highly conserved among several bacterial UPhs as well as in vertebrate UPhs (Pugmire & Ealick, 2002).

UPh has also been shown to be important in the activation and catabolism of fluoropyrimidines and modulation of its enzymatic activity may affect the therapeutic efficacy of these chemotherapeutic agents. UPh plays an important role in the homeostatic regulation of both intracellular and plasma uridine concentrations. Uridine plasma concentration is under very stringent regulation, mostly as a function of liver metabolic control, intracellular UPh enzymatic activity and cellular transport by both facilitated diffusion and Na^+-dependent active-transport mechanisms. Uridine is critical in the synthesis of RNA, the assembly of biological membranes through the formation of pyrimidine–lipid and pyrimidine–sugar conjugates, and the regulation of a number of biological processes.

UPh from *Salmonella typhimurium* (StUPh) contains 253 amino-acid residues. Comparison of the amino-acid sequences of StUPh and *Escherichia coli* UPh (EcUPh) shows them to be highly similar, with 97% identity (Zolotukhina *et al.*, 2003). The differing amino-acid residues are generally not involved in the active site of UPh; however, StUPh has a higher substrate specificity compared with its ortholog from *E. coli* (Molchan *et al.*, 1998). Although many purine nucleoside phosphorylase (PNP) structures have been reported (Bzowska *et al.*, 1995; Ealick *et al.*, 1990; Mao *et al.*, 1997; Shi *et al.*, 2001, 2004; Tebbe *et al.*, 1999), only the EcUPh structure has been published.

In this paper, we report the first three-dimensional X-ray structure of StUPh and only the second example of a member of the UPh family.

Table 1
Crystallographic data and data-collection statistics.

Values in parentheses are for the highest resolution bin.

Space group	$P6_1$ (No. 178)
Unit-cell parameters (Å)	a = 91.37, c = 266.38
Monomers per AU	6
X-ray source	X13 beamline, DESY, Hamburg
Wavelength (Å)	0.803
Resolution (Å)	28.34–2.5 (2.66–2.5)
No. of observations	160390
No. of unique reflections	42989 (6867)
Redundancy	3.73
Completeness (%)	99.2 (98.8)
Mosaicity (°)	0.62
Average $I/\sigma(I)$	13.31 (6.49)
$R_{\rm merge}$	7.3 (18.4)

Table 2
Refinement and final model statistics.

Values in parentheses are for the highest resolution bin.

Resolution range (Å)	28.34–2.5 (2.66–2.5)
No. of reflections in working set	40830 (6510)
No. of reflections in test set	2159 (357)
Data cutoff $\sigma(F)$	2
$V_{\rm M}$ (Å^3 Da^{-1})	2.01
Solvent content (%)	38.18
No. of amino-acid residues/atoms	1518/11256
No. of water molecules	168
No. of heteroatoms	10
$R_{\rm cryst}$ (%)	22.1 (31.9)
$R_{\rm free}$ (%)	27.9 (35.4)
Root-mean-square deviations	
Bond lengths (Å)	0.01
Bond angles (°)	1.50
B factor overall (Å^2)	47.7
Ramachandran plot statistics, residues in (%)	
Most favored regions	74.7
Additionally allowed regions	23.1
Generously allowed regions	2.2
Disallowed regions	0.0

2. Materials and methods

2.1. Purification, crystallization and X-ray data collection

StUPh was overexpressed in *E. coli* and purified by hydrophobic chromatography as described previously (Dontsova *et al.*, 2004; Mikhailov *et al.*, 1992; Molchan *et al.*, 1998). Fractions containing pure StUPh were pooled and dialyzed into buffer containing 10 m*M* Tris–HCl pH 7.3, 0.4% NaN_3 and concentrated to 20 mg ml^{-1}. Crystallization experiments were performed using the hanging-drop vapor-diffusion method on siliconized glass cover slides in Linbro plates at 294 K (Dontsova *et al.*, 2004). The reservoir solution contained 100 m*M* sodium acetate trihydrate pH 5.0, 7%(*w*/*v*) PEG 8000. The hanging drops contained 2.5 µl 20 mg ml^{-1} StUPh and 2.5 µl reservoir solution. Crystals appeared after 2–3 d and grew to maximum dimensions of 0.10 × 0.05 × 0.04 mm within one week. The crystals were transferred into 20% PEG 400, 100 m*M* sodium acetate trihydrate buffer pH 5.0 prior to flash-freezing in liquid nitrogen.

The crystals belong to space group $P6_1$, with unit-cell parameters a = 91.37, c = 266.38 Å, and diffract to 2.5 Å resolution. The Matthews coefficient (Matthews, 1968) calculated for one hexamer per asymmetric unit was 2.01 Å^3 Da^{-1}, which corresponds to a solvent content of 38%. X-ray intensity data were collected at 100 K at beamline X13 (EMBL/DESY, Hamburg, Germany). All data were processed and merged with the *DENZO* and *SCALEPACK* programs (Otwinowski & Minor, 1997). Data-collection and processing statistics are summarized in Table 1.

2.2. Structure determination

The crystal structure was solved by the molecular-replacement method using a medium-resolution structure of StUPh (PDB code 1ryz) as the search model. The amino-acid sequences were obtained from the SWISS-PROT data bank (CAA74658). The program *MOLREP* (Vaguine *et al.*, 1999) from the *CCP*4 suite gave a clear solution for one hexameric molecule of StUPh (Table 1). Following rigid-body refinement with *CNS* v.1.1 (Brünger *et al.*, 1998), the $R_{\rm cryst}$ for this model using all data to 2.5 Å converged to 42.8%.

2.3. Refinement

Noncrystallographic symmetry (NCS) restraints were used during the early stages of refinement, but were relaxed in the later stages. The structure was subjected to several rounds of simulated-annealing refinement using *CNS* (Brünger *et al.*, 1998) and manual model inspection and rebuilding using *O* (Jones *et al.*, 1991). A free *R* factor ($R_{\rm free}$), calculated from 5% of reflections set aside at the outset, was used to monitor the progress of refinement. The model bias present in the initial molecular-replacement solution was tackled using composite omit, cross-validated and σ_A-weighted maps as implemented in *CNS*. When the $R_{\rm cryst}$ value reached 30%, water molecules were placed into peaks greater than 3σ from ($|F_{\rm o}| - |F_{\rm c}|$) maps, but only when they were within a suitable hydrogen-bonding distance of protein atoms. After refinement, water molecules whose positions were not supported by the electron density at 1σ contouring in a σ_A-weighted ($|2F_{\rm o}| - |F_{\rm c}|$) map were deleted. The final model, refined to an $R_{\rm cryst}$ of 22.1% ($R_{\rm free}$ = 27.9%) at 2.5 Å resolution, showed good quality (Table 2) as judged with the program *PROCHECK* (Laskowski *et al.*, 1993) and had no residues in the disallowed regions of the Ramachandran plot (Ramachandran & Sasisekharan, 1968).

3. Results and discussion

3.1. Overall structure of StUPh

StUPh forms a symmetric doughnut-shaped homohexamer with a thickness of ∼51 Å and an outer diameter of ∼108 Å (Fig. 1). The overall structure is similar to the hexameric (high-molecular-weight) purine nucleoside phosphorylase family (Morgunova *et al.*, 1995). The hexamer has a central channel of about 19 Å diameter and a length of 30 Å. The channel narrows at one end to about 10 Å diameter and at the other end to about 16 Å diameter in the perpendicular direction.

The hexamer can be thought of as a trimer of dimers with 32 point-group symmetry. Each monomer in the hexamer makes a close contact with an identical one related by a twofold noncrystallographic axis, forming the pairs *AF*, *BD* and *EC*. These three dimers, which contain two complete active sites per dimer, pack together to form a hexamer using the threefold non-crystallographic axis that is perpendicular to the three twofold axes (Fig. 1). The interface region between the two monomers related by the threefold NCS comprises only hydrophobic residues, with a contact surface area of 2066 Å^2. The interface region generated by the twofold NCS comprises both hydrophobic interactions and hydrogen bonds for each dimer. In the *AF* dimer these hydrogen-bonding amino acids are Arg48*A*–Asp27*F*, Arg48*A*–Glu49*F*, Arg87*A*–Tyr172*F*, His122*A*–Thr161*F* and Ser173*A*–Gln209*F*. The contact area generated by the dimer interaction is 3303 Å^2. The monomers of the dimer pack together with an angle that is 3–4° less than the corresponding angle in EcUPh (Caradoc-Davies *et al.*, 2004).

The hexamers in the $P6_1$ crystal form are packed in layers involving both hydrophobic interactions and hydrogen bonds. Seven hydrogen bonds form in one layer and 16 hydrogen bonds form in the other

(Table 3). The area of contact is about 3600 Å^2 per hexamer for each side. The crystal structure gives independent results for each of the six monomers (labeled *A*–*F*) for a total of 11 434 non-H atoms.

3.2. Structure of the StUPh monomer

The StUPh monomer belongs to the large class of α/β proteins. The fold of the StUPh monomer has a three-layer ($\alpha\beta\alpha$) sandwich architecture reminiscent of a modified Rossmann fold. The monomer of StUPh has a central 11-stranded mixed β-sheet core consisting of strands β2-β3-β4-β1-β5-β11-β6-β7-β8-β9-β10, flanked by six α-helices (Fig. 1). The overall structure of StUPh is very similar to the structures of EcUPh and EcPNP (Mao *et al.*, 1997) and retains the topology of the hexameric NP-I enzymes as described by Pugmire & Ealick (2002). Thus, the bacterial UPhs and high-molecular-weight bacterial PNPs show significant structural homology, having a hexameric quaternary structure, a similar overall fold and similar sizes and positions of the secondary-structural elements. The main structural difference between hexameric UPhs and PNPs lies in the region of residues 160–178 in EcUPh and StUPh (Caradoc-Davies *et al.*, 2004). In PNP, this region comprises a short stretch of three amino-acid residues (163–165) that leads from the loop linking β7 to α5. In UPhs, this segment includes an additional 14 amino-acid residues to form an extended loop which folds over the surface of the adjacent monomer.

Table 3
Intermolecular hydrogen bonds.

Residue	Monomer	Residue	Monomer
Side 1			
Asn14	*A*	Asp170	A
Arg212	*A*	Gln226	A
Arg212	*A*	Glu227	*A*
Tyr172	*D*	Asn103	*C*
Tyr169	*E*	Asp5	*E*
Glu186	*F*	Gln226	*C*
Gln226	*F*	Glu186	*C*
Side 2			
Asp170	*A*	Asn14	*A*
Thr171	*A*	Asn14	*A*
Glu185	*A*	Thr171	*F*
Gln226	*A*	Gln20	*A*
Glu227	*A*	Arg212	*A*
Gly174	*B*	Gln225	*F*
Gly174	*B*	Glu227	*F*
Asn222	*B*	Glu232	*F*
Thr224	*B*	Asn230	*F*
Asn103	*C*	Tyr172	*D*
Tyr169	*C*	Tyr169	*F*
Tyr169	*C*	Arg175	*F*
Glu186	*C*	Gln226	*F*
Gln226	*C*	Glu186	*F*
Asn230	*C*	Tyr169	*D*
Glu232	*C*	Glu167	*D*
Asp5	*E*	Tyr169	*E*
Asn14	*E*	Ser173	*E*

3.3. Active site

The active site for EcUPh includes amino acids from two subunits (Caradoc-Davies *et al.*, 2004; Morgunova *et al.*, 1995). This region of StUPh (using the *BD* dimer as representative) contains a phosphate ion, which contacts amino acids Arg91*B*, Arg30B, Thr94*B*, Gly26*B*, Glu198*B* and Arg48*D* (monomers *B* and *D* are related by twofold NCS; Fig. 2). The positions of residues are similar to the corresponding amino acids in EcUPh (Caradoc-Davies *et al.*, 2004). Therefore, it is likely that the ribose-binding and pyrimidine base-binding sites also resemble the corresponding sites in EcUPh. Consequently, for the *BD* dimer the ribose-binding site includes Glu198*B*, Arg91*B*, Met197*B* and His8*D* and the pyrimidine base-binding site includes Gln166*B*, Arg168*B*, Arg223*B* (hydrogen bonds) and Ile220*B* and Val22*B* (hydrophobic interactions).

Open, intermediate and closed active-site conformations have been described for EcUPh based on the position of residues in the loop 219–239. The open active site was observed when no substrates were bound and the intermediate and closed active-site conformations were found when substrates were bound to the monomers. Superposition of monomers from EcUPh and StUPh shows that StUPh contains only the open conformation of the active site. Therefore, the presence of a phosphate ion does not appear to influence the conformational state of the active-site loop.

In future experiments we plan to obtain the X-ray structure for native StUPh at higher resolution and to determine the structures of

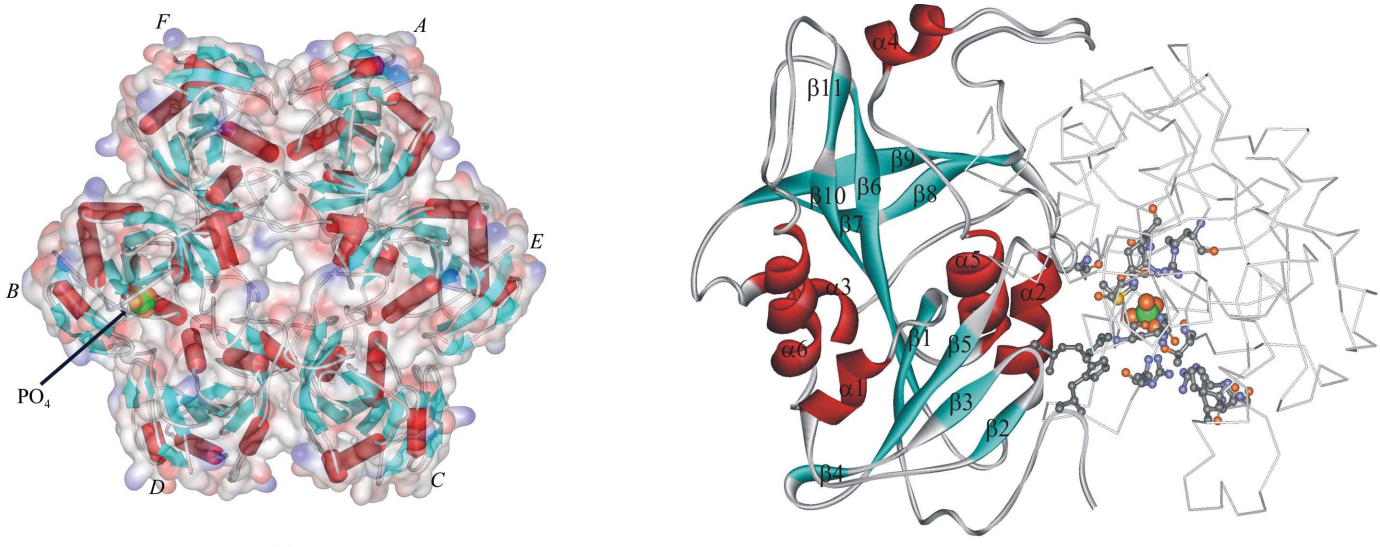

(*a*) (*b*)

Figure 1
The structure of StUPh. (*a*) Electrostatic surface diagram with the structure of the hexamer color-coded by the secondary-structural elements. (*b*) A pair of twofold-related monomers forming a complete active site. One monomer is shown with a ribbon diagram color-coded by secondary-structural elements. The other monomer is shown as a backbone trace with the active-site residues and the phosphate ion shown in ball-and-stick representation.

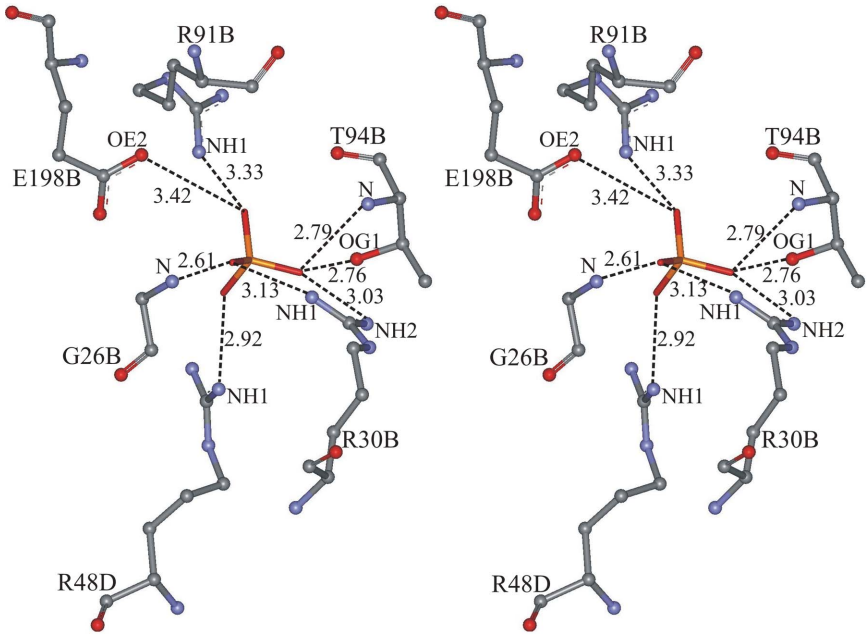

Figure 2
Stereoview showing the site of connection with the orthophosphate ion in the *BD* active dimer of StUPh.

StUPh with bound ligands in order to better understand the biological function of this enzyme.

This investigation was supported by BMBF (Bundesministerium fur Forschung and Wissenschaft under contract No. RUS/214), a grant from the Program on Molecular and Cellular Biology RAS (No. 10002-251/π-10/145-161/140503-085) and an RFBR (Russian Foundation for Basic Research) grant No. 04-02-97213. Support for this project was also provided by a grant to SEE (2U19CA67763) from the National Institutes of Health.

References

Brünger, A. T., Adams, P. D., Clore, G. M., DeLano, W. L., Gros, P., Grosse-Kunstleve, R. W., Jiang, J.-S., Kuszewski, J., Nilges, M., Pannu, N. S., Read, R. J., Rice, L. M., Simonson, T. & Warren, G. L. (1998). *Acta Cryst.* D**54**, 905–921.
Bzowska, A., Luic, M., Schroder, W., Shugar, D., Saenger, W. & Koellner, G. (1995). *FEBS Lett.* **367**, 214–218.
Caradoc-Davies, T. T., Cutfield, S. M., Lamont, I. L. & Cutfield, J. F. (2004). *J. Mol. Biol.* **337**, 337–354.
Dontsova, M. V., Savochkina, Y. A., Gabdoulkhakov, A. G., Baidakov, S. N., Lyashenko, A. V., Zolotukhina, M., Errais Lopes, L., Garber, M. B., Morgunova, E. Y., Nikonov, S. V., Mironov, A. S., Ealick, S. E. & Mikhailov, A. M. (2004). *Acta Cryst.* D**60**, 709–711.
Ealick, S. E., Rule, S. A., Carter, D. C., Greenhough, T. J., Babu, Y. S., Cook, W. J., Habash, J., Helliwell, J. R., Stoeckler, J. D., Parks, R. E. Jr, Chen, S. & Bugg, C. E. (1990). *J. Biol. Chem.* **265**, 1812–1820.
Jones, T. A., Zou, J.-Y., Cowan, S. W. & Kjeldgaard, M. (1991). *Acta Cryst.* A**47**, 110–119.
Laskowski, R. A., MacArthur, M. W., Moss, D. S. & Thornton, J. M. (1993). *J. Appl. Cryst.* **26**, 283–291.
Mao, C., Cook, W. J., Zhou, M., Koszalka, G. W., Krenitsky, T. A. & Ealick, S. E. (1997). *Structure*, **5**, 1373–1383.
Matthews, B. W. (1968). *J. Mol. Biol.* **33**, 491–497.
Mikhailov, A. M., Smirnova, E. A., Tsuprun, V. L., Tagunova, I. V., Vainshtein, B. K., Linkova, E. V., Komissarov, A. A., Siprashvili, Z. Z. & Mironov, A. S. (1992). *Biochem. Int.* **26**, 607–615.
Molchan, O. K., Dmitrieva, N. A., Romanova, D. V., Lopes, L. E., Debabov, V. G. & Mironov, A. S. (1998). *Biochemistry (Mosc.)*, **63**, 195–199.
Morgunova, E. Y., Mikhailov, A. M., Popov, A. N., Blagova, E. V., Smirnova, E. A., Vainshtein, B. K., Mao, C., Armstrong, S. R., Ealick, S. E., Komissarov, A. A., Linkova, E. V., Burlakova, A. A., Mironov, A. S. & Debabov, V. G. (1995). *FEBS Lett.* **367**, 183–187.
Otwinowski, Z. & Minor, W. (1997). *Methods Enzymol.* **276**, 307–326.
Pugmire, M. J. & Ealick, S. E. (2002). *Biochem. J.* **361**, 1–25.
Ramachandran, S. & Sasisekharan, V. (1968). *Adv. Protein Chem.* **23**, 283–437.
Shi, W., Basso, L. A., Santos, D. S., Tyler, P. C., Furneaux, R. H., Blanchard, J. S., Almo, S. C. & Schramm, V. L. (2001). *Biochemistry*, **40**, 8204–8215.
Shi, W., Ting, L. M., Kicska, G. A., Lewandowicz, A., Tyler, P. C., Evans, G. B., Furneaux, R. H., Kim, K., Almo, S. C. & Schramm, V. L. (2004). *J. Biol. Chem.* **279**, 18103–18106.
Tebbe, J., Bzowska, A., Wielgus-Kutrowska, B., Schroder, W., Kazimierczuk, Z., Shugar, D., Saenger, W. & Koellner, G. (1999). *J. Mol. Biol.* **294**, 1239–1255.
Vaguine, A. A., Richelle, J. & Wodak, S. J. (1999). *Acta Cryst.* D**55**, 191–205.
Zolotukhina, M., Ovcharova, I., Eremina, S., Errais Lopes, L. & Mironov, A. S. (2003). *Res. Microbiol.* **154**, 510–520.